

AURORAL TOMOGRAPHY ANALYSIS OF A FOLDED ARC OBSERVED AT THE ALIS-JAPAN MULTI-STATION CAMPAIGN ON MARCH 26, 1995

Takehiko ASO¹, Masaki EJIRI¹, Akira URASHIMA², Hiroshi MIYAOKA¹,
Åke STEEN³, Urban BRÄNDSTRÖM³ and Björn GUSTAVSSON³

¹*National Institute of Polar Research, 9–10, Kaga 1-chome,
Itabashi-ku, Tokyo 173-8515*

²*Department of Electrical Engineering, Kyoto University, Kyoto 606-8501*

³*Swedish Institute of Space Physics, P.O. Box 812, S-981 28 Kiruna, Sweden*

Abstract: Auroral tomography is a state-of-the-art method to retrieve three dimensional (3D) structure of luminous aurora from images taken simultaneously at multiple observation points. Imaging is basically monochromatic and altitude structures as well as horizontal vortex structures at particular wavelength are reconstructed. These are crucial for quantitative understanding of auroral formation and dynamical processes. In March 1995, the first multi-point international campaign between Sweden and Japan was carried out using three unmanned Swedish ALIS stations (Kiruna, Merasjärvi, Tjautjas) and two Japanese sites (Abisko, Nikkaluokta), separated by about 50 km in Kiruna region. ALIS stands for the Auroral Large Imaging System which aims at capturing large-scale composite auroral images as well as optical tomographic imaging by a computer-controlled networking.

In this paper, a description is given on the analysis of auroral tomography on the reconstruction of folded auroral arc observed at 2340:30 UT on March 26, 1995. The images are taken for 1–5 s integration at a green line of 557.7 nm. Cameras were pointed to one of the preset common field of view, *viz.*, a core region which is just overhead of Kiruna. Optical tomography relying on inversion analysis by the algebraic reconstruction technique has been carried out. The result indicates a fold structure of auroral arc with inferred altitude profile of photo-emission peaking at around 120 km.

1. Introduction

The 3D luminous structure of aurora reflects physical and dynamical process of auroral formation and its perturbation occurring at particle source and acceleration regions and the ionosphere. Application of computed tomography (CT; used in various fields such as medical diagnosis or seismology) to auroral physics has been discussed in ASO *et al.* (1990) as a reasonable extension of the 2D reconstruction of aurora based on binocular stereopsis. Aurora stereoscopic observations were to determine the altitude of lower edge of auroral curtain by a triangulation (STENBAEK-NIELSEN and HALLINAN, 1979) and then to infer 2D or limited 3D structure of volume luminosity (ASO *et al.*, 1990, 1993, 1994, FREY *et al.*, 1996). Also, a scanning photometer chain was used to estimate the contour structure of luminosity in the magnetic meridian plane (ROMICK and BELON, 1967; VALLANCE JONES *et al.*, 1991)

In Kiruna, the Swedish Institute of Space Physics has been constructing the ALIS (an acronym for Auroral Large Imaging System) which is a network of unmanned aurora imaging equipments linked together under a computer network (STEEN, 1989; STEEN *et al.*, 1990; STEEN and BRÄNDSTRÖM, 1993). The network obtains a composite large-scale auroral image with fairly high temporal resolution, and also, by adjusting vergence angles, captures images of common field of view for 3D auroral tomography. At the moment, three ALIS stations were established and JICCD (Japanese ICCD) cameras (ASO *et al.*, 1993, 1994) are set up at two other sites; this enabled us to carry out the first multi-point tomographic observation with 5-point ALIS-Japan collaborative network.

Numerical tests are carried out both for the feasibility of reconstruction and for the evaluation of analyzed auroral structures. The result of these tests gives a measure of retrieval (or more definitely its uniqueness) for the number and relative locations of observing sites for the model aurora which is based on the actually observed aurora.

Tomographic images taken at 2340:30 UT on March 26, 1995 are analyzed using a SIRT (Simultaneous Iterative Reconstruction Technique) algorithm (GILBERT, 1972) with some plausible constraint on the field-alignedness of auroral formation. The reconstruction shows a vortex structure with complex folding, and the altitude profile of the luminosity is found to be compared reasonably with results calculated under given assumptions. This indicates that the auroral tomography can well delineate the 3D structure of auroral luminosity from the data at a limited number of stations, with some reasonable assumptions for solving this underdetermined inverse problem.

2. Tomographic Analysis

Tomographic images are first calibrated in orientation by using star images taken separately for each camera pointing directions. This gives a relation of pixel coordinate with the azimuth and elevation of corresponding line-of-sight. Imaging characteristics of $2 \sin(\theta/2)$, where θ is the angle relative to the optical axis, are found to hold for JICCD cameras, while $\theta + 2 \tan \theta$ approximates the ALIS cameras. Optical axis direction is estimated by a non-linear least squares method using the Levenberg-Marquardt algorithm, assuming a polynomial approximation of perspective projection to observed star images (Aso *et al.*, 1990). Fields of view for the JICCD and ALIS cameras are about 90° and 60° , respectively. Gray levels should be corrected for limb darkening, taking account of optical characteristics together with phosphor light calibration images and approximate flat field images. Atmospheric absorption or multiple scattering is not considered at present.

For the JICCD cameras, temperature control was not so strict, and amplification factors of an image intensifier varies with temperature change. Hence, the relative sensitivity is also a parameter in the iteration procedure stated below.

In the present analysis, volume cells (voxels) with assigned luminosity value are assumed in the auroral region. A modified version of the SIRT is used. The method updates voxel values by reflecting all projection values pertinent to the voxel. A formula for this algorithm is expressed as

$$\tilde{L}_j^{(k+1)} = \tilde{L}_j^{(k)} \prod_i \left(\frac{g_i}{\tilde{g}_i^{(k)}} \right)^{\lambda \cdot w_{ij} / \sum_i w_{ij}}, \quad (1)$$

where L_j is the luminosity of voxel j , w_{ij} weighs how the voxel j contributes to the gray level g_i of the pixel i , λ is a relaxation parameter to adjust revision steps, and k is the iteration number. This formulation shows that each voxel value is augmented multiplicatively with the averaged weight if the observed value g_i is greater than the reconstructed gray level \tilde{g}_i and *vice versa*. Initial guess for these voxel values is set to be uniform.

One important constraint for this underdetermined inverse problem is that the luminosity obeys the identical field-aligned profile at nearby or proximate voxels. We call this to be a proximity-constraint as formulated by

$$\tilde{L}^{(k+1)}(x', y', z') = \frac{\iint \tilde{L}^{(k)}(x', y', w) dw \int \tilde{L}^{(k)}(x' - u, y' - v, z') dudv}{\int \iint \tilde{L}^{(k)}(x' - u, y' - v, w) dudvdw}. \quad (2)$$

Here, x', y', z' is a coordinate system along the geomagnetic line of force with z' taken along it and horizontal (x', y') has the same value for each geomagnetic field-line (YABU *et al.*, 1993). In the above calculation, altitude profiles along the geomagnetic line of force for the nearby cells are averaged and cell values are redistributed along each line of force, scaling it to the integrated values along it. In other words, this postulates that the auroral formation is basically along the geomagnetic line of force with slowly varying field-aligned profiles.

Iterations go on for 60–70 for the present analysis until \tilde{g}_i becomes close to g_i in a least squares sense. Gray levels in each image used for reconstruction are sampled by the epipolar line constraint so as to secure common field of view, and to eliminate artifacts occurring at the edge of relevant reconstructed region.

3. Numerical Simulation

Numerical tests for this underdetermined inverse problem are necessary for evaluating the reliability of inferred reconstruction. Here, the auroral model shown in Fig. 1a is created based on the observed and then reconstructed luminous structure of an aurora arc with a simple fold at 1909:30 UT on the same day (Aso *et al.*, 1998). Figure 1b illustrates the cross-correlation of model and reconstructed voxel values versus numbers and combinations of observing sites. A broken line is a result with a proximity constraint, whereas a solid line is by the modified SIRT only. By and large, the reconstruction is better for larger number of sites. It is, however, evident that the station 5, north of the arc, plays a dominant contribution and even a 5-point observation, *e.g.* (1,2,3,4,6) gives less reliable result than the 4-point one (1,4,5,6) which includes the station 5. Slight degradation in (1,2,4,6) relative to (1,4,6), in (1,2,3,4,6) relative to (1,3,4,6) or in (1,2,4,5,6) relative to (1,4,5,6) is due to the increase in reconstructed volume which is only in sight from 1 and 2, and due to fair reconstruction in this region. Also, the proximity constraint is found to be very efficient even for the 2-point observation so long as the aurora conforms to the involved assumption of iden-

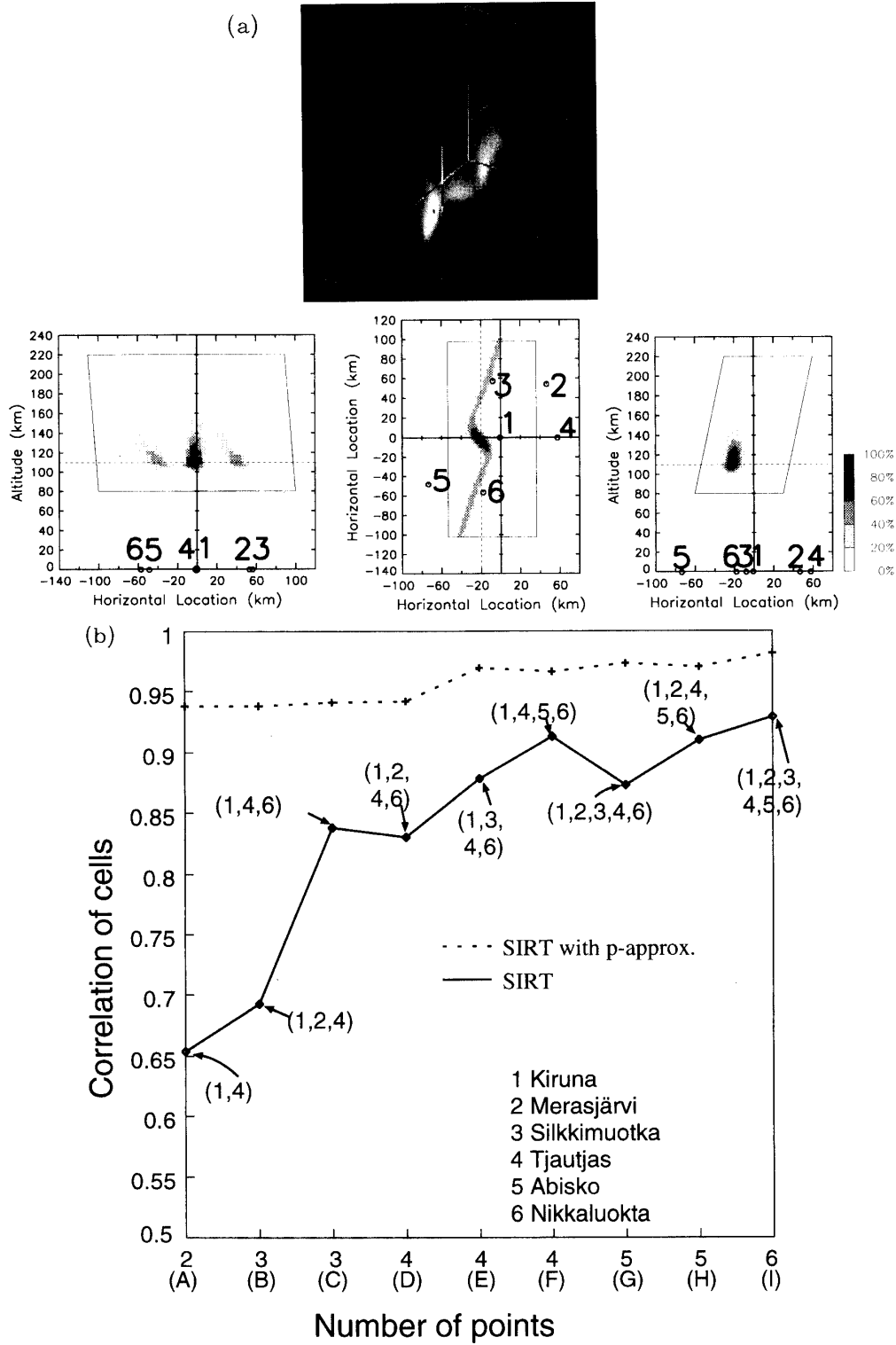


Fig. 1. (a) Aurora model with a fold illustrated by 3D visualization and three sectional contours. (b) Cross-correlation of reconstructed and modelled luminosity voxels versus number and combinations of sites for SIRT reconstruction with (broken line) and without (solid line) a proximity constraint.

tical field-aligned profile in its proximity.

4. Observation

Figure 2 illustrates the 557.7 nm monochromatic images taken at three ALIS stations, Tjautjas, Kiruna, Merasjärvi and one Japanese site, Nikkaluokta. Camera pointing, image taking and house keeping for ALIS are controlled remotely from Kiruna and all cameras are in the core direction. All ALIS images are taken by a bare CCD detector with 16 bits/pixel image field of 1024×1024 pixel resolution at 5 s exposure time. This quad output CCD camera ensures fast read-out time with fairly low read-out noise. On the other hand, the JICCD at Nikkaluokta captured a 512×512 image of 8 bits/pixel resolution at 1 s averaging. Voltage control for image intensifier and interference filter change were manually performed. In this example, aurora motion is relatively slow and blurring in ALIS images compared to 1 s averaged Nikkaluokta image is not evident. So, it is assumed that aurora form was stable during 5 s of image integration in estimating body structure of aurora in the present analysis.

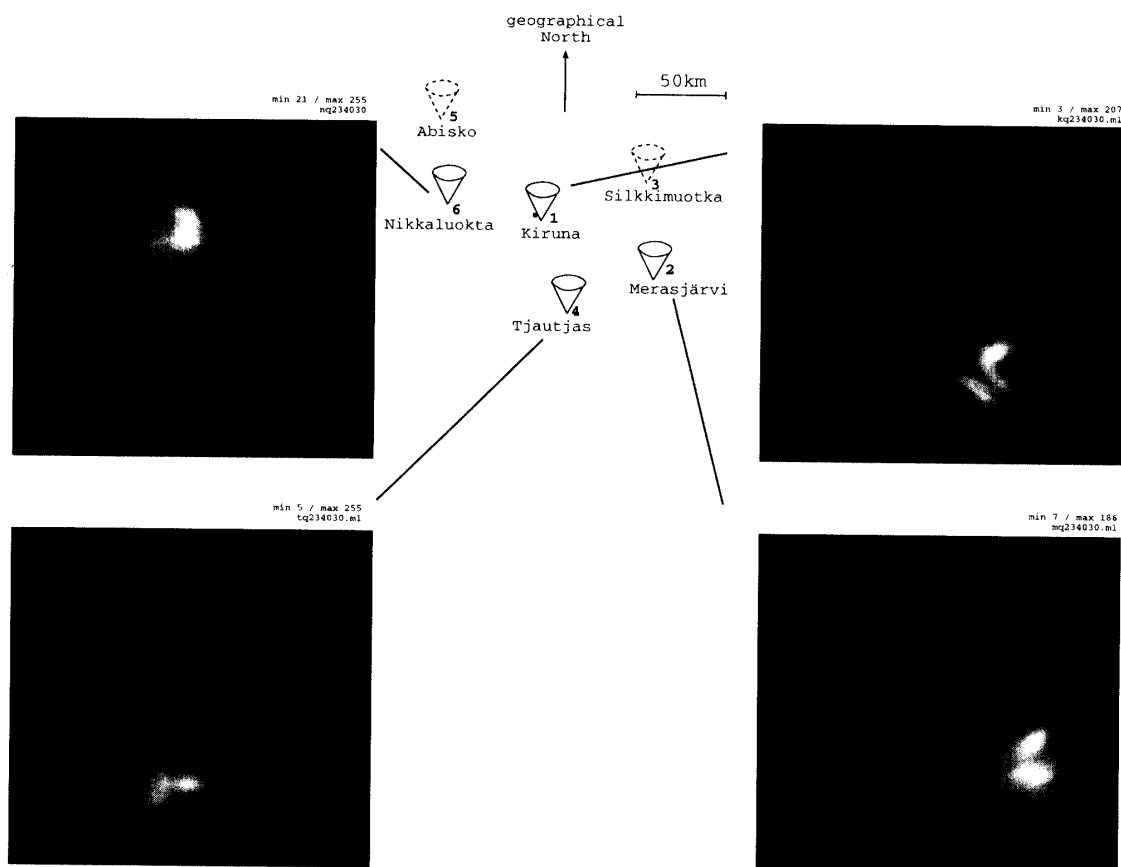


Fig. 2. Tomographic images at 2340:30 UT, March 26, 1995 taken at Nikkaluokta (top left), Tjautjas (bottom left), Kiruna (top right) and Merasjärvi (bottom right) and the locations of observing sites in the ALIS network.

5. Results and Discussions

These CT images are analyzed by the modified SIRT method stated above. Voxels are assumed in this region from 80 to 220 km in altitude, 90–120 km in NS and 200 km in EW directions. Voxel numbers are $70 \times 45 \sim 60 \times 50$ with a size of 2 km in altitude and thickness (NS) and 4 km in extended (EW) directions. Relative sensitivity in gray level is varied as a parameter so that residuals $\tilde{g}_i - g_i$ are minimized. This is required as the JICCD cameras are not fully calibrated for temperature fluctuations as stated before.

In this reconstruction, uniform initial guess is given to all cells. A proximity con-

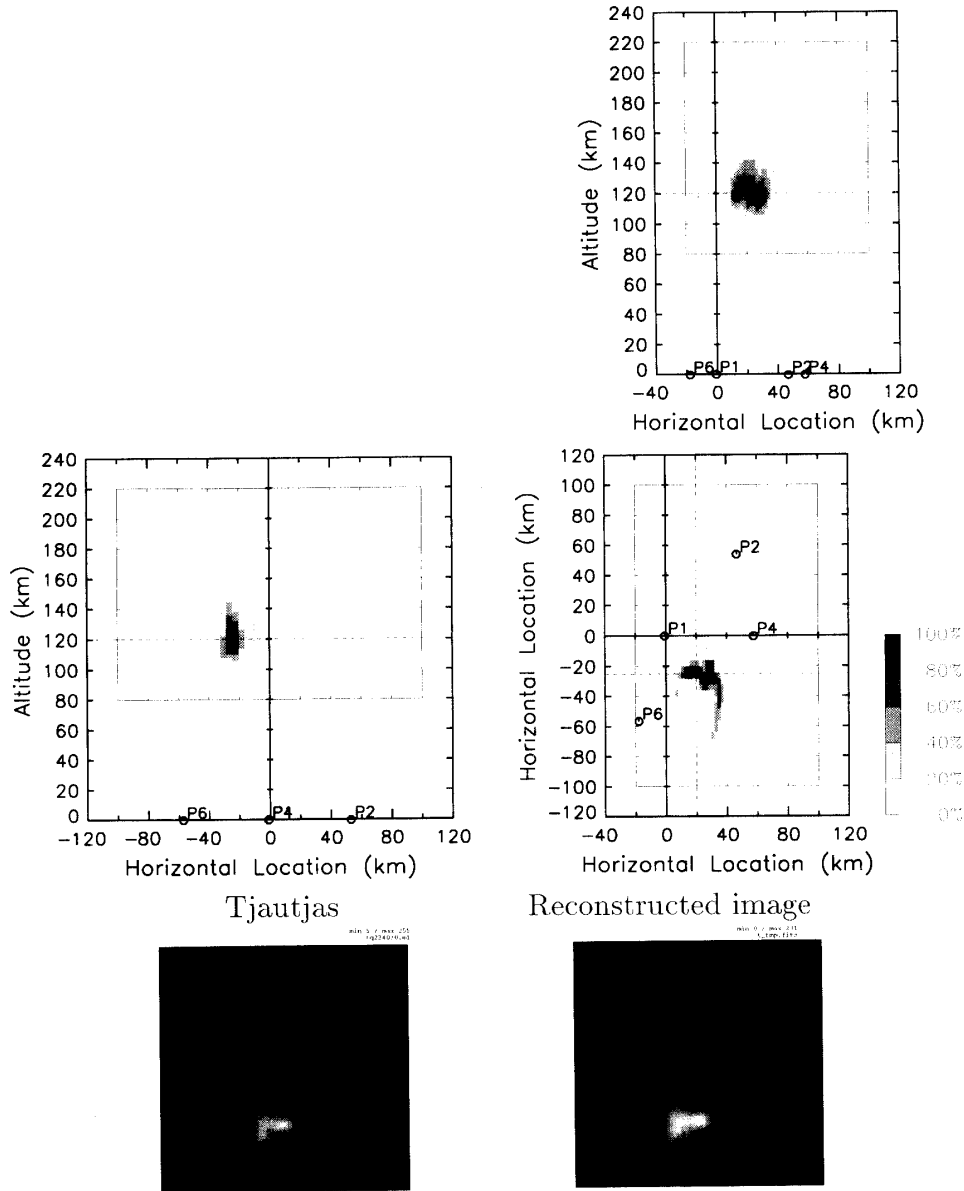


Fig. 3. Shaded contours of the reconstructed aurora. A broken line in each figure indicates the section where other contours are shown. An altitude profile in the meridian plane (top) shows a structure at a fold, and horizontal plan (middle right) indicates how the vortex looks like. Lower image pair compares the observed (left) and reconstructed images at Tjautjas.

straint is added in which altitude profiles along the geomagnetic line of force for the nearby ± 8 cells in NS and ± 4 cells in EW are averaged. Cell values are redistributed according to eq. (2). The SIRT iteration is then resumed, and the sequence is repeated until the residual becomes a minimum.

Figure 3 shows shaded contours of the reconstructed structure in three sections, meridian plane (top right), horizontal plan (middle right) and east-west plane (middle left). A broken line in each section indicates where corresponding contour is depicted. An altitude profile in the meridian plane shows a structure at a fold, and horizontal plan indicates how the vortex is undulated. An image pair at the bottom compares the observed (left) and reconstructed images seen from Tjautjas. It is seen that projected images are at least very similar to each other with disparity of about 10%

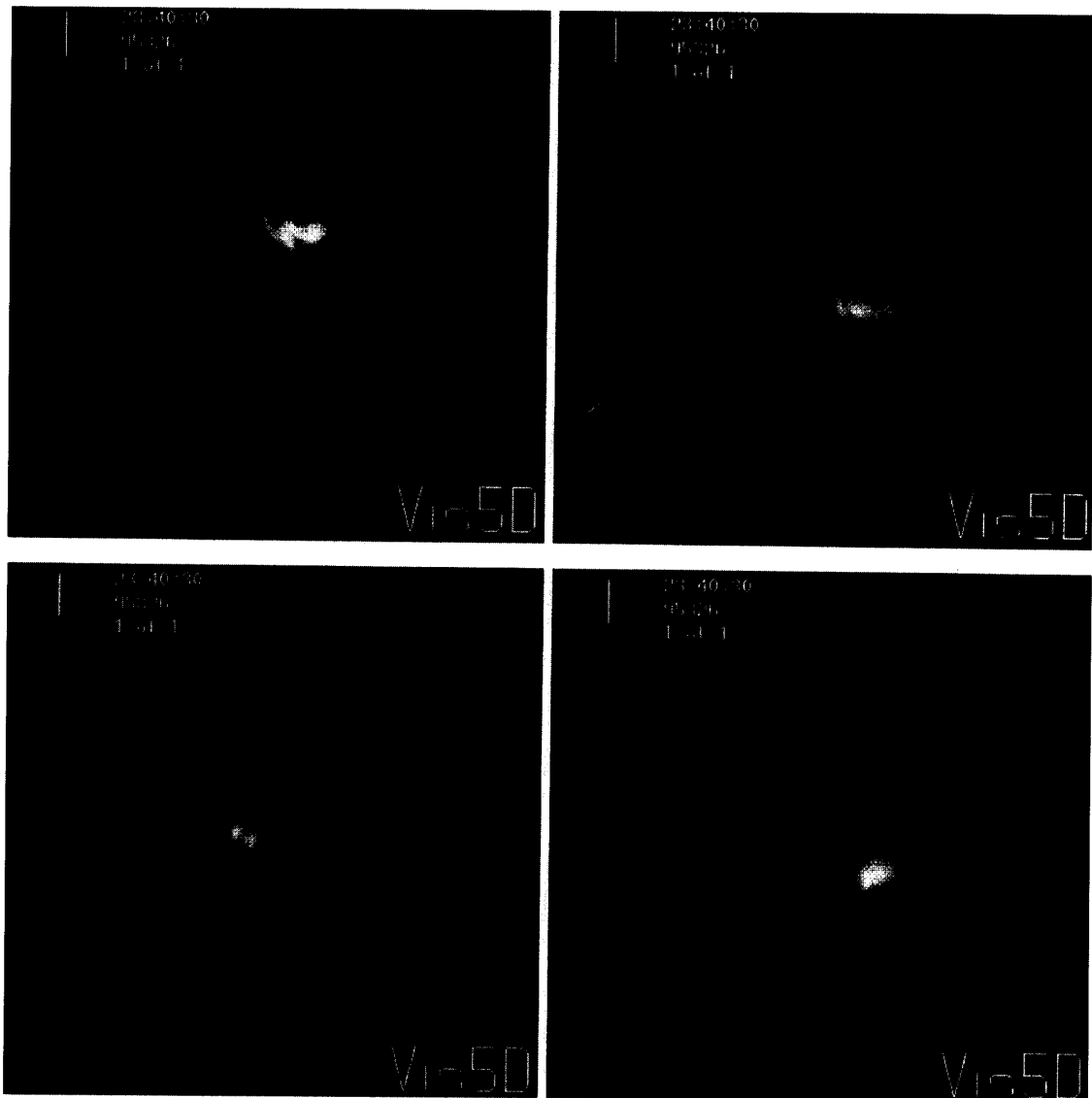


Fig. 4. Four visualizations of reconstructed aurora. A box is 140 km in altitude with 120 km in NS and 200 km in EW directions. A program Vis5D is by courtesy of Dr. William L. HIBBARD, University Wisconsin-Madison.

or less in the present reconstruction.

3D visualization of the reconstructed aurora as seen from four directions are shown in Fig. 4. These are produced by Vis5D program supplied by courtesy of Dr. William L. HIBBARD at the University of Wisconsin–Madison. A letter N denoted at a tick in the middle of a lower edge of a box designates the north direction. From these results, it is seen that the auroral curtain folds with enhanced luminosity in the middle. The altitude of this enhanced region is around 120 km and east-west extension of a fold is of the order of 20 km. The retrieved thickness in the almost meridional plane is about 10–20 km. A vortex structure thus reconstructed could be interpreted by future conjunction observations with the EISCAT radar and polar satellites as in the work by STEEN *et al.* (1988). As a matter of fact, observations of electron density and electron and ion temperature increases, electric field and drift velocity by radars as well as *in-situ* measurement of impinging particles are requisite to elucidating perturbation of auroral structures. A comparison will be made also with the numerical modelling of auroral formation now under intensive study by ONDA *et al.* (1998).

Figure 5 shows a reconstructed altitude profiles of auroral luminosity in the midst of a folded arc. The emission rate is in arbitrary and linear scale. These are field-aligned profiles for the geomagnetic line of force passing through the points whose coordinates (x , y , z) are shown in the figure. x and y refer to NS and EW horizontal axis, respectively, and z is altitude as illustrated in Fig. 3. It is seen that, though the quenching below the peak at around 120 km is less rapid, the inferred result com-

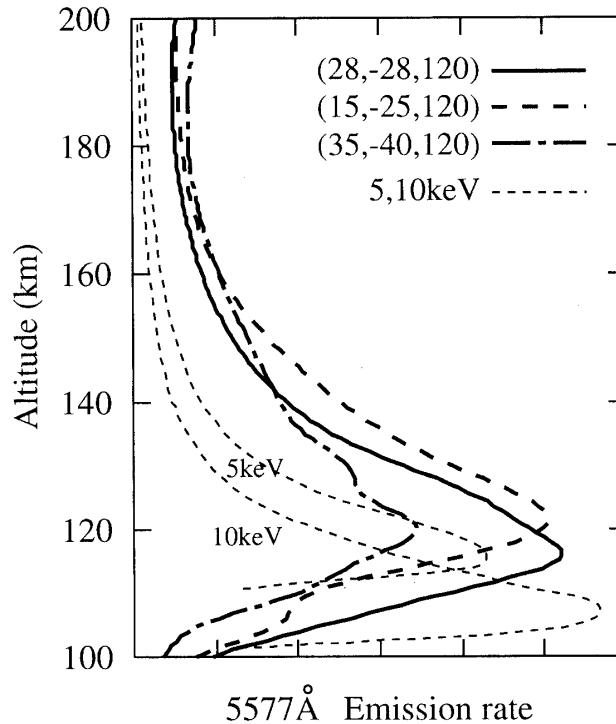


Fig. 5. Reconstructed emission profiles observed at 2340:30 UT, March 26, 1995 and theoretical emission profiles at 557.7 nm by monoenergetic 5 and 10 keV electrons by BANKS and CHAPPEL (1974).

pare reasonably with theoretical emission profile at 557.7 nm by monoenergetic electrons by BANKS and CHAPPEL (1974). The energy of electrons impinging on atomic oxygen is inferred to be some 5 keV or less in the present arc structure.

In the present tomographic data, the temporal and spatial resolutions are some 5 s and several km corresponding to voxel size. The sensitivity of cameras can capture enhanced auroras with exposure time of 1 s or less. As the number of imaging sites increases, better spatial resolution is to be anticipated with limitation due to the pixel resolution.

6. Conclusion

In this paper, an example analysis is given for a folded aurora arc above the 4-point observing network. A modified SIRT method is used along with an assumption of field-alignedness which might be a basic nature of auroral arc formation. Aurora shows a vortex structure of complex fold which awaits further studies with the EISCAT radar and the polar satellite data. The result presented here serves to indicate a promising application of computed tomography to the study of 3D aurora structure from ground based multi-point observations.

Acknowledgments

The authors gratefully acknowledge supports by the Grant-in-Aid for Scientific Research (No.07640588) from the Ministry of Education, Science and Culture, Japan and by the Research Grant-in-Aid for FY 1994 from the Tateisi Science and Technology Foundation.

References

- ASO, T., HASHIMOTO, T., ABE, M., ONO, T. and EJIRI, M. (1990): On the analysis of aurora stereo observations. *J. Geomagn. Geoelectr.*, **42**, 579–595.
- ASO, T., EJIRI, M., MIYAOKA, H., ONO, T., HASHIMOTO, T., YABU, T. and ABE, M. (1993): Aurora stereo observation in Iceland. *Proc. NIPR Symp. Upper Atmos. Phys.*, **6**, 1–14.
- ASO, T., EJIRI, M., MIYAOKA, H., ONO, T., YABU, T., MUGURUMA, K., HASHIMOTO, T. and ABE, M. (1994): Aurora stereo observation in Iceland and its tomography analysis. *Trans. Inst. Electronics Communication Engineers, D-II*, J77-D-II(1), 69–78 (in Japanese).
- ASO, T., EJIRI, M., URASHIMA, A., MIYAOKA, H., STEEN, A., BRÄNDSTRÖM, U. and GUSTAVSSON, B. (1998): First results of auroral tomography from ALIS-Japan multi-station observations in March 1995. *Earth, Planets Space*, **50** (in press).
- BANKS, P. M. and CHAPPEL, C. R. (1974): A new model for the interaction of auroral electrons with the atmosphere: Spectral degradation, backscatter, optical emission, and ionization. *J. Geophys. Res.*, **79**, 1459–1470.
- FREY, S., FREY, H. U., CARR, D. J., BAUER, O. H. and HAERENDEL, G. (1996): Auroral emission profiles extracted from three-dimensionally reconstructed arcs. *J. Geophys. Res.*, **101**, 21731–21741.
- GILBERT, P. (1972): Iterative methods for the three-dimensional reconstruction of an object from projections. *J. Theor. Biol.*, **36**, 105–117.
- ONDA, K., EJIRI, M., ITIKAWA, Y. and MIYAOKA, H. (1998): Altitude profile of electron density and oxygen green line in active auroral arcs based on electron differential number flux observed by sounding rocket. *Proc. NIPR Symp. Upper Atmos. Phys.*, **11**, 36–54.

- ROMICK, G. J. and BELON, A. E. (1967): The spatial variation of auroral luminosity -II. *Planet. Space Sci.*, **15**, 1695–1716.
- STEEN, A. (1989): ALIS—An Auroral Large Imaging System in Northern Scandinavia. *Proc. Ninth ESA/PAC Symposium on 'European Rocket and Balloon Programmes and Related Research'*, Lahnstein, FRG, 299–303.
- STEEN, A. and BRÄNDSTRÖM, U. (1993): ALIS—A multi-station ground-based imaging system at high latitudes. *STEP Int. Newsl.*, **3**(5), 11–14.
- STEEN, A., COLLIS, P. N. and HÄGGSTRÖM, I. (1988): On the development of folds in auroral arcs. *J. Atmos. Terr. Phys.*, **50**, 301–313.
- STEEN, A., BRÄNDSTRÖM, U. and KAILA, K. (1990): A scientific and technical description of ALIS. *Proc. NSSR Annual Meeting*, Bolkesjö, Norway, 153–164.
- STENBAEK-NIELSEN, H. C. and HALLINAN, T. J. (1979): Pulsating auroras: Evidence for noncollisional thermalization of precipitating electrons. *J. Geophys. Res.*, **84**, 3257–3271.
- VALLANCE JONES, A., GATTINGER, R. L., CREUTZBERG, F., HARRIS, F. R., MCNAMARA, A. G., YAU, A. W., LLEWELLYN, E. J., LUMMERZHEIM, D., REES, M. H., MCDADE, I. C. and MARGOT, J. (1991): The ARIES auroral modelling campaign: Characterization and modelling of an evening auroral arc observed from a rocket and a ground-based line of meridian scanners. *Planet. Space Sci.*, **39**, 1677–1705.
- YABU, T., ASO, T., HASHIMOTO, T., ABE, M. and EJIRI, M. (1993): An upgraded method for reconstructing 3-dimensional structure of aurora from stereo images. *Nankyoku Shiryô (Antarct. Rec.)*, **37**, 231–251 (in Japanese with English abstract).

(Received April 16, 1997; Revised manuscript accepted June 23, 1997)